Natural Hazards
and Earth System
Sciences
Discussions

Discussion Paper | Discussion Paper | Discussion Paper | Discussion Paper |

Calibration of FARSITE fire area simulator in Iranian northern forests

R. Jahdi[1], M. Salis[2,3], A. A. Darvishsefat[1], F. J. Alcasena Urdiroz[3,4], V. Etemad[1], M. A. Mostafavi[5], O. M. Lozano[2], and D. Spano[2,3]

[1]University of Tehran, Faculty of Natural Resources, Zobe Ahan Street, Area Code 3158777878, P.O. BOX 4314, Karaj, Iran
[2]University of Sassari, Department of Science for Nature and Environmental Resources (DIPNET), Via Enrico De Nicola 9, 07100, Sassari, Italy
[3]Euro-Mediterranean Center for Climate Changes (CMCC), IAFENT Division, Via De Nicola 9, 07100, Sassari, Italy
[4]University of Lleida (UdL), School of Agricultural Engineering (ETSEA), Agriculture and Forest Engineering Department, Alcalde Rovira Roure 191, 25198, Lleida, Spain
[5]Center for Research in Geomatics (CRG) 1055, avenue du Séminaire, Pavillon Louis-Jacques Casault, Université Laval, Québec, G1V 0A6, QC, Canada

Abstract

Wildfire simulators based on empirical or physical models need to be locally calibrated and validated when used under conditions that differ from those where the simulators were originally developed. This study aims to calibrate FARSITE fire spread model considering a set of recent wildfires occurred in Northern Iran forests. Site specific fuel models in the study areas were selected by sampling the main natural vegetation type complexes and assigning standard fuel models. Overall, simulated fires presented reliable outputs that accurately replicated the observed fire perimeters and behavior. Standard fuel models of Scott and Burgan (2005) afforded better accuracy in the simulated fire perimeters than the standard fuel models of Anderson (1982). The best match between observed and modeled burned areas was observed on herbaceous type fuel models. Fire modeling showed a high potential for estimating spatial variability in fire spread and behavior in the study areas. This work represents a first step in the application of fire spread modeling on Northern Iran for wildfire risk monitoring and management.

1 Introduction

Wildfires cause substantial losses in ecosystems and valued resources in Iran as well as all around the world (Keeley and Fotheringham, 2001; Pausas et al., 2008; Banj Shafiei et al., 2010; Bracmort, 2012). Every year, about 6000 ha of forests are burned in Iran (FAO, 2005), and almost 7 % of this area is located in the northern Iranian mountainous range (Banj Shafiei et al., 2010). Wildfires in Northern Iran forests are mostly caused by anthropogenic activities, as well as in other areas (Syphard et al., 2007; Bird et al., 2008; Romero-Calcerrada et al., 2008; Martinez et al., 2009) and represent the main threat in the protected natural areas. The North Iran mountainous forests have a very high natural value and correspond to the main habitat for many protected, endangered and endemic animals, such as the Iranian

cheetah (*Acinonyx jubatus venaticus* Hilzheimer, 1913), the Persian fallow deer (*Dama dama mesopotamica* Brooke, 1875), the Persian ground jay (*Podoces pleskei* Zarudny, 1896), the Caucasus leopard (*Panthera pardus ciscaucasica* Satunin, 1914), lynx (*Lynx lynx* Linnaeus, 1758), brown bear (*Ursus arctos syriacus* Hemprich and Ehrenberg, 1828), wild boar (*Sus scrofa* Linnaeus, 1758), wolf (*Canis lupus* Linnaeus, 1758), golden jackal (*Canis aureus* Linnaeus, 1758), jungle cat (*Felis chaus* Schreber, 1777), badger (*Meles meles* Linnaeus, 1758), and plants, like the Persian ironwood (*Parrotia persica* C.A. Mey.), Caspian beech (*Fagus orientalis* Lispsky), the velvet maple (*Acer velutinum* Boiss.) and the Caspian locust (*Gleditsia caspica* Desf.), among many others.

As pointed out by several previous works, wildfire spread is a complex spatial and temporal dynamic process that depends on many factors such as weather, topography, fuel types and fuel moisture content (Carvalho et al., 2006; Santoni et al., 2011; Salis et al., 2014a). The ability to analyze and quantify potential wildfire likelihood, size and intensity is important for an effective wildfire management and proactive emergency response (Gu et al., 2008; Taylor et al., 2013; Ager et al., 2014a). For this reason, several surface fire spread models have been developed under many conditions in different areas around the world, particularly where wildfires are threatening forests, valued resources and human lives (Sullivan, 2009). These models are implemented for simulating complex physical-chemical and dynamic processes over large and spatially heterogeneous landscapes, under changing weather and fuel moisture conditions (Finney, 1998; Sullivan, 2009).

Fire modeling has been extensively applied in the last decades to simulate and characterize fire spread and behavior across diverse types of landscapes (Arca et al., 2007; Duguy et al., 2007; Ager et al., 2011, 2014b; Salis et al., 2013, 2014b). Many wildfire simulators have been developed since the 90's, as SIROFIRE (Australia; Coleman and Sullivan, 1996), FARSITE (United States; Finney, 1998), PROMETHEUS (Canada; Prometheus Project Steering Committee, 1999), SPREAD (Portugal; Mendes-Lopes and Aguas, 2000) and ForeFire (France; Balbi et al., 2009),

among others. FARSITE is a spatially and temporally explicit fire simulation system developed at the USDA Forest Service, Fire Sciences Laboratory of Missoula, and is still nowadays one of the most used and user friendly simulators. The simulator is a semi-empirical model based on Rothermel's (1972) surface fire spread model, simulates fire growth using Huygens's principle wave propagation and fire intensity is calculated from Byram's (1959) equation. FARSITE has been widely calibrated in the US and employed not only to generate spatial maps of fire spread and behavior (Finney and Ryan, 1995; Finney, 1998), but also mainly to evaluate the effects of different silvicultural prescriptions and fuel treatment options on reducing fire hazard (Stephens, 1998; Finney, 2001; Stratton, 2004; LaCroix et al., 2006; Ryu et al., 2007; Schmidt et al., 2008; Cochrane et al., 2012). However, the use of FARSITE simulator on areas different from those ones where the model was originally developed requires a local calibration and validation (Arca et al., 2007) using observed real wildfire data, and corresponds to the primary step to then apply the simulator at larger scales (Ager et al., 2007, 2010; Stratton, 2006; Salis et al., 2013, 2014b). The reliability of FARSITE as a tool for improving wildfire analysis and landscape management options has been reported by several papers in southern Europe (Molina and Castellnou, 2002; Arca et al., 2007; Duguy et al., 2007; Mallinis et al., 2008; Glasa and Halada, 2011), as well as in New Zealand, Australia (Opperman et al., 2006) and southeast Asia (Lee et al., 2010). Nevertheless, no studies have been carried out with FARSITE in Iran and the surrounding countries of southwest Asia.

FARSITE requires a set of geospatial data concerning topography, surface fuel models and canopy characteristics derived from GIS or remote sensing, as well as the physical parameters of the fuel bed, fuel moisture content, and weather data: the outputs of fire spread models strongly depend on the quality of the above mentioned input data, especially as far as weather data and fuel models are concerned (Arca et al., 2007). Although data availability increased during the recent years, fuel maps still result difficult to be generated and updated in many regions of the world, due to the absence of specific geospatial fuel model cartography or the lack of employable

information on mapped vegetation attributes (Pettinari et al., 2013). In the last years several studies developed photo-guides and collections of fuel models (Anderson, 1982; Dimitrakopoulos, 2002; Scott and Burgan, 2005; Fernandes et al., 2006; Cruz and Fernandes, 2008; Rodríguez y Silva and Molina-Martínez, 2011; Cai et al., 2014; Pierce et al., 2014). Standard fuel models that fit the main local vegetation complexes or fuel types properties can become as input for fire spread modeling, also in combination with custom fuel models whenever available (Duguy et al., 2007; Arca et al., 2009; Boboulos et al., 2013).

In this paper, we assessed the capabilities of FARSITE in accurately replicating wildfire spread and behavior in northern Iran. We tested different standard fuel models (Anderson, 1982; Scott and Burgan, 2005) in order to identify the ones that better replicate and fit the observed fire events. In addition, how selected fire spread and behavior variables (rate of spread, fireline intensity, and flame length) were influenced by standard fuel models is also analyzed. This work represents the first study aiming at calibrating and validating FARSITE in northern forests of Iran. The study improves our understanding of the potential fire spread and behavior in the southern Caspian forests and can help landscape managers for several fire management purposes.

2 Materials and methods

2.1 Study area

This study was carried out considering a set of fires that occurred in southern Caspian forests of northern Iran, specifically in the Siahkal forest area and in the Golestan National Park (GNP) (Fig. 1). The south Caspian forests (16 481.95 km^2) cover about 1.2 % of the whole Iran (Marvi Mohadjer, 2005) and range from sea level to 2500 m (Siadati et al., 2010). Such area presents contrasted bioclimatic differences in comparison with the central and southern parts of the country, which are characterized by xeric dominant weather conditions.

The Siahkal forest area (about 1050 km^2) is located in Guilan Province in north Iran, in the western part of the South Caspian forest belt (Fig. 1). The annual precipitation ranges from 600 mm in the southern part to 2000 mm in the northern and highest mountains, and most of the annual rainfall occurs in autumn. Air relative humidity exceeding 80 % is responsible of frequent fogs at higher altitudes. Average minimum temperatures of the coldest month are commonly higher than the freezing point (0 °C) (Akhani et al., 2010). The forests, which form a long and narrow vegetation belt on the northward slopes of the Alborz Mountains, constitute the main representative of the Euro-Siberian flora in Iran (Djamali et al., 2009). The highest proportion (46 %) of the Siahkal area is covered by forests, which are dominated by temperate broad-leaved deciduous trees and are characterized by many thermophilous Tertiary relict species such as *Zelkova carpinifolia* (Pall.) K. Koch, *Parrotia persica* (DC.) C.A. Mey., *Pterocarya fraxinifolia* (Lam. ex Poir.) Spach, *Quercus castaneifolia* C.A. Mey., and Asian subtropical trees such as *Diospyros lotus* L., *Gleditsia caspica* L., *Danaë racemosa* (L.) Moench and *Albizzia julibrissin* Durazz. (Akhani, 1998; Akhani and Ziegler, 2002; Leestmans, 2005; Leroy and Arpe, 2007).

The Golestan National Park (GNP) is situated in northeast Iran, east of Golestan, northwest of North Khorasan and north of Semnan Provinces, and covers about 920 km^2 of land (Fig. 1). The National Park is located in a transitional position between the sub-humid south Caspian region and the semi-arid zones of central and east-central Iranian Plateau. The GNP ranges from 450 to 2400 m a.s.l. The wet air masses from the Caspian Sea are blocked by the high mountain ranges, which create particular microclimatic conditions, with annual precipitation ranging from 150 mm in the southeast up to more than 1000 mm in some central parts of the GNP (Akhani, 1998). The Park exhibits a diverse mosaic of vegetation units, including the Hyrcanian low to high altitude mesophytic forests, shrublands, open and closed scrub sometimes mixed with C4-grasslands, Juniperus woodlands, mountain steppes and meadows, Artemisia and Artemisia–Stipa steppes and different transitional and halophilous communities (Akhani, 1998; Akhani and Ziegler, 2002).

2.2 Wildfire history

In the period 2000–2011, Northern Iran experienced on average about 400 fires per year with about 2000 ha of area burned. The yearly fire trends, in terms of both number of fires and burned areas, are characterized by the presence of critical years (2006 and 2010) with respect to the ordinary trends (Fig. 2). Large and extreme fires in the study areas are commonly linked to drought conditions, heat waves, strong winds and fine dead fuel accumulation. As many as 90 % of the fires in the area are caused by humans (Sarkargar Ardakani, 2007; Zarekar et al., 2013; Mirdeylami et al., 2014; Iranian Forest Brigades, personal communication, 2011, 2012). Fires in northern Iran commonly occur during the short drought season in autumn, characterized by hot and dry winds that desiccate the forest understory. These conditions mostly lead to low-intensity surface fires, which rarely exceed 10–30 cm in flame height (Adel et al., 2012).

Wildfires in the Golestan National Park, as well as in the Siahkal forests, are distributed from March to December, with the peak of ignitions and area burned in June and November (Fig. 3). During the period 2000–2011, the Siahkal area experienced about 13 fires per year, with about 60 ha burned (Department of Forestry, Natural Resources Office, Guilan, Iran; Fig. 2). Approximately 85 % of the fires burned less than 10 ha; a small amount of fires (about 15 %) is responsible of half of the area burned (Fig. 4). No fires larger than 100 ha were observed in the studied period. On the other hand, in the Golestan National Park, in the period 2000–2011 about 12 fires per year have been recorded, with about 200 ha burned (Golestan National Park fire reports, personal communication; Fig. 2). In this area, the largest fires (> 100 ha) accounted for about 15 % of the total number, and were responsible of almost 75 % of the total area burned (Fig. 4).

2.3 Case studies

FARSITE simulations were run to simulate spread and behavior of four wildfires that affected the study areas during the 2010 and 2011 fire seasons: Toshi and Malekroud

fires in Siahkal forest, and YekeBermagh and Gharangi fires in the Golestan National Park (Fig. 1). Species and structural characteristics of vegetation for the different case studies are summarized in the Table 1. For all case studies, ignition locations and real fire perimeters were determined by survey fieldwork and Global Positioning System (GPS) data, as well as considering the information obtained from reports and interviews to forest rangers, firefighters and Park managers.

The Toshi wildfire occurred near the village of Toshi (lat. 37°11′ N, long. 49°88′ E), on August 2010, and burned about 34 ha of land (Fig. 5; Table 1). The fire started at 04:00 p.m. and lasted approximately 25 h. The ignition point was located near a steep slope, in an agricultural area (Fig. 5). About 16.4 ha were covered by mixed dense woodland of *Carpinus betulus* L., *Quercus castaneifolia* C.A. Mey., *Alnus subcordata* C.A. Mey., *Parrotia persica* C.A. Mey. and *Acer insigne var. velutinum* Boiss. Grasslands (*Asperula odorata* L., *Euphorbia helioscopia* L. and *Hypericum androsaemum* L.) covered about 13.4 ha of the area burned, and grass-shrublands characterized the remaining 4.7 ha of the area burned (Fig. 5). The weather was characterized by maximum temperature of 35 °C, average relative humidity of 50 %, and northeast winds (Table 2). The fire spread towards south-east, driven by the wind and the topographic conditions.

The Malekroud wildfire occurred near the town of Malekroud (lat. 37°03′ N, long. 49°84′ E), on December 2010, and burned approximately 24 ha in a low elevation area (Fig. 5; Table 1). The fire started at 5.00 p.m. near a road along the southern border of the fire perimeter. It spread for 15 h and was extinguished by the Forest firefighters after 17 h near a road, along the northern border of the fire perimeter (Fig. 5). The burned area was covered by timber litter fuel types with heterogeneous structural characteristics, and was mainly composed by *Acer insigne var. velutinum* Boiss., *Quercus castaneifolia* C.A. Mey., *Fagus orientalis* Lipsky. and *Alnus subcordata* C.A. Mey. The day of the fire was characterized by moderate maximum temperature (around 25 °C), average relative humidity of 58 % and southern winds. The fire moved towards north, driven by the mild slope and the wind.

The YekeBermagh wildfire occurred in the southern part of the Golestan National Park (lat. 37°22′ N, long. 56°03′ E). The wildfire was ignited at 11:00 a.m. on July 2011, and was extinguished at 09:00 p.m. (Fig. 5; Table 1). The northern part of the YekeBermagh area is characterized by a flat topography, while the southern part has a more complex and steep terrain with high spatial and temporal variability in wind speed and direction. Most of the 60 ha burned were covered by grasslands (*Festuca drymeia* Mert. & Koch., *Centaurea golestanica* Akhani & Wagenitz., *Artemisia sieberi* Besser. and *Astragalus jolderensis* B. Fedtsch). Juniperus woodlands, grass-shrublands composed by montane *Juniperus excelsa* M. Bieb. in steep slopes and subalpine *Juniperus communis* L. on exposed high slopes (Akhani, 1998) were also affected by the fire. The day of the fire the weather was hot (31 °C maximum temperature) and dry (21 % relative humidity). Fire spread was driven by the topography and the southwestern winds.

The Gharangi wildfire occurred on March 2011, in the southern part of the Golestan National Park (lat. 37°21′ N, long. 56°02′ E), and burned about 10 ha, from 02:00 to 09:00 p.m. (Fig. 5; Table 1). The area presents a mountainous orography with an altitude range between 1200 and 2160 m a.s.l. The vegetation burned was dense-mixed woodland, mainly composed by *Quercus castaneifolia* C.A. Mey.,*Carpinus betulus* L.,*Carpinus orientalis* Mill. and *Acer cappadocicum* Gled. The weather was relatively moderate, with maximum air temperature of 17 °C and average relative humidity of 49 %. The fire spread towards north-east driven by moderate south-east winds. The fire intensity was low due to the shielding effect of the dense and closed canopy.

2.4 Fuel mapping and fuel model assignments

Fuel models and canopy characteristics maps were produced by intensive field sampling and measurements on the main plant communities of the study areas, in combination with the 1 : 25 000 land-cover maps (Department of Forestry, Natural Resources Office, Guilan, and Department of Environment, Golestan, Iran). The field activities were carried out due to the lack of detailed vegetation information on forest

and shrubs characteristics and types for the study areas. The field samplings were conducted following the Line Transect method (Marshall et al., 2000, 2003), with the objective of measuring the surface fuel model parameters and canopy characteristics. On the whole, 21 line transects with a distance of 150 m in Siahkal forests and 25 line transects with a distance of 100 m in the GNP were used. Square shape vegetation sampling plots, with 1 m × 1 m size for grass fields and 10 m × 10 m size in woodlands, were used to sample the vegetation characteristics. The vegetation data concerning to fuel bed depth, vegetation composition, structural stage, canopy height and crown base height were gathered, as well as photographs, in Global Positioning System (GPS) georeferenced 188 and 250 plots, respectively in Siahkal area and Golestan National Park. Visual estimations were used to assign a canopy cover class (< 1 %, 1–5 %, 6–10 %, 11–25 %, 26–50 %, 51–75 % and 76–100 %) in every plot. Then the experiences of fire engineers were collected in order to generate fuel model maps and photo guides in conjunction with the georeferenced sampling data (Anderson, 1982; Scott and Burgan, 2005; Table 3; Fig. 6) that allowed us reinterpreting the initial vegetation maps. In this study, USDA standard fuel models were selected based on the similarities between the vegetations structure characteristics observed in the field and the standard models of Anderson (1982) and Scott and Burgan (2005).

In particular, GR4, GR6 and GR7 (Table 3; Scott and Burgan, 2005), as well as FM2 and FM3 (Table 3; Anderson, 1982) standard fuel models were used to represent grass-dominated fuel beds (GR; Fig. 6). GS1, GS2 and GS3 (Table 3; Scott and Burgan, 2005), and also FM5 and FM6 (Table 3; Anderson, 1982) standard fuel models were assigned to vegetation presenting a mixture of grass and shrub components (GS; Fig. 6). SH1 and SH2 (Table 3; Scott and Burgan, 2005) fuel models were assigned to areas where shrubs covered at least 50 % of the surface, with sparse grassland among shrubby patches (SH; Fig. 6). In forested areas with grass-shrub and litter mixed understory, TU1, TU2, TU3 and TU5 (Table 3; Scott and Burgan, 2005) models were used (TU; Fig. 6). Models TL6 and TL9 (Table 3; Scott and Burgan, 2005) covered dead and downed woody fuels beneath forest canopies (TL; Fig. 6). FM8, FM9, and

FM10 (Table 3; Anderson, 1982) covered timber litter, hardwood litter, and litter and understory. NB1, NB3, NB8, and NB9 standard fuel models (Scott and Burgan, 2005) were assigned respectively for urban areas, ploughed agricultural lands, water bodies and bare ground, in the Siahkal area (Fig. 5). Non burnable fuels corresponding to roads, buildings and urban areas were extracted from the 1 : 25 000 digital topographic maps (National Cartographic Centre of Iran).

2.5 Input data for fire simulations

FARSITE requires spatial grids of topography (slope, aspect and elevation), surface fuels (fuel model) and fuels canopy characteristics (stand height, crown base height, crown bulk density, canopy cover) as basic inputs for the simulations. These data layers were assembled in a landscape file (LCP), with 10 m resolution. Topography layers were derived from the digital elevation model (DEM) (National Cartographic Centre of Iran, NCC) for each case study. As previously described, surface and crown fuels layers were derived from land cover maps and field sampling.

Weather data of the day of the fire, corresponding to hourly air temperature, relative humidity, wind speed, wind direction and rainfall, were collected from the nearest weather stations to the wildfire case studies (Fig. 5 and Table 2).

Initial fuel moisture content (FMC) for the 1, 10, and 100 h dead fuels (Table 3) was determined following the methodology proposed by Rothermel (1983). With this method, we estimated the fine dead FMC for each case study, and then we derived 10 and 100 h dead moisture by adding 2 and 4 % respectively to the 1 h dead FMC (Hardison, 2003). The live herbaceous and woody FMC values (Table 3) were estimated from literature data (Arca et al., 2007; Sağlam et al., 2008; Chuvieco et al., 2011) and field observations.

2.6 FARSITE simulations

FARSITE simulations were run at 10 m of resolution, using different combinations of standard fuel models (Anderson, 1982; Scott and Burgan, 2005) for the main fuel types (grasslands, grass-shrublands, shrublands, timber understory, and timber litter) affected by the real fires (Table 5). With this approach, we assessed the diverse influence of fuel models on fire perimeter accuracy and on potential fire behavior.

For all simulations and fuel models, the adjustment factor for the fire spread rate was set at 1.0. Real suppression activities were not considered in the simulations as well as spot and crown fires, since both were not observed in the case studies presented in this paper. Ignition location and fire spread duration used as inputs for each case study are provided in Table 1.

Vector files of the simulated fire perimeters and gridded data of simulated rate of spread (ROS), fireline intensity (FLI) and flame length (FML) were exported and analyzed in GIS environment. As previously pointed out, the gridded data outputs were exported at 10 m resolution, for each case study.

2.7 Statistical analysis

The simulation performances with different combinations of fuel models were evaluated for all the case studies (Table 5). An error matrix between actual and simulated fire perimeters was calculated to define the frequency of each case (presence/absence of burned areas). Sorensen's coefficient (SC; Legendre and Legendre, 1998) and Cohen's Kappa coefficient (K; Congalton, 1991) were used as measures of the accuracy of the extent of the fire spread (Arca et al., 2007; Salis, 2008).

Sorensen's coefficient (SC) is an indicator of the exclusive association between observed and simulated burned areas. SC values were calculated as follows:

$$SC = \frac{2a}{2a + b + c},$$

where a is the number of cells coded as burned in both observed and simulated data, b is the number of cells coded as burned in the simulation and unburned in the observation, and c is the number of cells coded as unburned in the simulation and burned in the observation (Arca et al., 2007).

5 Kappa statistics (K) computes the frequency with which simulated area agrees with observed area; with an adjustment that takes into account agreement by chance (Filippi et al., 2014). K values were calculated as follows:

$$K = \frac{N \sum_{i=1}^{r} x_{ii} - \sum_{i=1}^{r}(x_i + x_{+i})}{N^2 - \sum_{i=1}^{r}(x_{i+} x_{+i})},$$

10 where r is the number of rows in the matrix, x_{ii} is the number of observations in row i and column i, x_{i+} and x_{+i} are the marginal totals of row i and column i, respectively, and N is the total number of observations. Both K and SC coefficient values typically range between zero and one, with values close to one indicating very high agreement between simulated and observed fire perimeters (Arca et al., 2007).

15 Due to differences in fuel models characteristics, the simulations revealed diverse potential fire behavior. The Zonal Statistics tool of ArcGis 10 was used to analyze and summarize the fire behavior data (ROS, FLI and FML; Table 6) for each fuel model.

3 Results

3.1 Fire simulation accuracy

20 For all the case studies, the simulated burned areas were compared with the observed fire perimeters (Fig. 7 and Tables 4 and 5). Overall, the statistics showed that the best FARSITE performances were obtained for all the case studies using the standard fuel models of Scott and Burgan (2005), with the exception of the simulation II of Malekroud, where the standard fuel model (FM9) of Anderson (1982) showed the best accuracy in 25 replicating the fire perimeter (Table 4).

In the Toshi fire event, the best results were obtained in the simulation I (Fig. 7a, Table 4), where about 30.1 ha of the final fire area coincided with the actual fire area, while 4.1 and 5.5 ha were respectively underestimated and overestimated by FARSITE. As previously pointed out, the best values of SC and K coefficients were obtained in the 5 simulation I (SC = 0.86, K = 0.82; Table 4), whereas the other simulations presented lower accuracies, with SC values ranging from 0.48 to 0.81, and K values from 0.45 to 0.79. The best performance for Toshi wildfire, regarding the standard fuel models used, was obtained by the GR6 fuel model (SC = 0.92, K = 0.87; Table 5) for grasslands and the worst was observed for the TU3 fuel model (SC = 0.75, K = 0.73; Table 5). Overall, 10 in the Toshi wildfire statistical tests showed a good accordance between actual and simulated fire areas.

The simulation II of Malekroud wildfire event (Fig. 7b, Table 4) replicated well the observed fire event, with an agreement between the observed and simulated fire area of about 20.6 ha and FARSITE underestimation and overestimation of 3.5 and 5.5 ha 15 respectively. The statistical analysis showed that the FM9 fuel model in simulation II provided the highest SC and K values (SC = 0.85; K = 0.82; Table 5), while the other simulations using TL6 and FM10 fuel models gave SC values ranging from 0.73 and 0.78 and K values ranging from 0.71 and 0.75 (Table 4). Focusing on single fuel models, the FM9 fuel model in Toshi case study provided the worst accuracy 20 performance (SC = 0.48; K = 0.45; Table 4).

In the simulation V of the YekeBermagh case study (Fig. 7c, Table 4), the simulated fire area was characterized by an overestimation of 30.7 ha, mainly in the right back-flank of the fire spread. The agreement between the simulated and observed fire area was about 46.8 ha, while 11.2 ha of the fire area were underestimated (Table 4). The 25 statistical test showed that in the simulation V the GR4 fuel model provided the best SC and K values (SC = 0.82, K = 0.81; Table 5), while the worst performances were provided by the FM2 fuel model in the simulation VI (SC = 0.13, K = 0.12; Table 4), due to the wide underestimation of the area burned. The large underestimation was also confirmed for the FM5 and FM6 fuel models.

In the simulation I of Gharangi wildfire event (Fig. 7d, Table 4), about 7.5 ha of the observed fire area were correctly simulated as burned area by FARSITE. The extent of the underestimation by the simulation was approximately 2.6 ha, and the overestimation 2.2 ha. The best agreement between simulated and observed fire was linked to TL9 fuel model (SC = 0.91; K = 0.91; Table 5), which was characterized by small overestimation and underestimation of the FARSITE perimeter.

Comparing the standard fuel models associated to the best simulations of FARSITE for each case study, the higher SC and K values were obtained using the GR6 grassland model in the simulation I of the Toshi fire (SC = 0.92; K = 0.87; Table 5) and the TL9 timber model in the simulation I of the Gharangi fire (SC = 0.91, K = 0.91; Table 5). The worst performances were provided by the model TU1 in the simulation I of Gharangi fire event (SC = 0.47; K = 0.45; Table 5). On the whole, GR6, TU2, TU5 and TL9 fuel models replicated well the observed area burned (SC $\geq$ 0.90 and $K \geq$ 0.82; Table 5).

3.2 Fuel models and fire behavior

Surface fire rate of spread (ROS, m min^{-1}), fireline intensity (FLI, kW m^{-1}), and flame length (FML, m) were analyzed for each of the fuel models used in the four case studies (Fig. 8 and Table 5). The fire simulation outputs showed complex patterns that were generally related to the dominant fuel types and to topography.

Overall, the wind speed conditions were not too strong for the case studies presented, and for this reason the fires spread slowly and the ROS was not high, especially in the Gharangi wildfire.

The highest values of simulated ROS were observed with tall and dense grasslands and sparse shrubland vegetation in Toshi and YekeBermagh case studies (Table 5). The grasslands presented the fastest rate of spread, which varied from 0.05 to 10.84 m min^{-1} (Table 5) depending on topography; the shrublands showed rate of spread ranging from 0.05 to 8.06 m min^{-1} (Table 5). The lowest ROS (< 1 m min^{-1}; Table 5) were obtained for the areas covered by mixed hardwood forest (TU1) and

pure hardwood forest (TL6) in Gharangi wildfire. In woodlands, modeled fire rate of spread was very slow due to the high fuel compactness and the relatively high moisture content: this explains the ROS values 2 ∼ 3 times lower than in grassland fuel types (Table 5).

As well as rate of spread, relevant differences in terms of fireline intensity between grasslands and other vegetations were identified. The grass fuel models presented the highest fireline intensity (> 350 kW m^{-1}; Table 5). The higher fireline intensity values were also associated to shrubland fuel models (SH1 and SH2; > 250 kW m^{-1}; Table 5) in YekeBermagh wildfire case study. Moreover, in woodlands the flame length was short (< 1 m; Table 5) compared to other vegetation types, while the longest flame values were obtained for tall grasslands (> 1 m; Table 5).

4 Discussion

The propagation of a wildfire depends on complex interaction among terrain, fuel types, weather conditions, fire suppression, and the fire itself (Viegas et al., 1998; Forthofer and Butler, 2007; Fernandes, 2009; Lee et al., 2010; Sharples et al., 2012; Cardil et al., 2013). The use of fire spread models can help understanding the expected fire behavior and play a key role in proactive decision-making to take decisions before the fire front arrival. Nevertheless, fire spread model adoption and application should be preceded by a calibration protocol, as well as a verification that demonstrates that the model outcomes represent the processes they aim to describe within acceptable error bounds (Stratton, 2006; Arca et al., 2007; Randall et al., 2007; Alexander and Cruz, 2013). In fact, modeling fires is difficult due to a myriad of causes, including spatial heterogeneity in environmental factors and the variable effects of fire suppression over the range of fire sizes (Taylor et al., 2013). On the other hand, validation and calibration of fire simulations in general is also made difficult by the multiple sources of errors that are confounded with the error of the model itself. These include the accuracy of spatial fuels information, bias in weather station locations compared to where the fire is burning, and

mapping of fire perimeter locations, errors from the user who runs the models (Finney et al., 2011).

The goal of this manuscript was to assess the capabilities of FARSITE in replicating wildfire spread and behavior in northern Iran, where the number of scientific studies and projects on fire behavior and spread are still limited. Plenty of studies on these topics have been carried out in the United States, southern Europe and other Mediterranean areas, and local site-specific fuel models have been developed and widely employed in fire modeling (Finney, 1998, 2003; Finney et al., 2006; Scott and Burgan, 2005; Santoni and Balbi, 1998; Arca et al., 2007, 2009; Fernandes et al., 2006; Salis et al., 2010, 2013, 2014b). Albeit standard fuel models should not be applied uncritically to ecosystems outside of North America, this study showed that standard fuel models can accurately replicate fire perimeters and behavior in our study areas. In this work, the main fuel model types and characteristics were initially identified by classifying the vegetation structures combining field sampling data and bibliographic information (Anderson, 1982; Scott and Burgan, 2005). Then, we associated each fuel type to a specific standard fuel model to simulate fire propagation and behavior with FARSITE (Finney, 1998). The results highlighted that some standard fuel models accurately replicated the observed burned areas and fire behavior in the Hyrcanian forests.

The good agreement between the actual and simulated fire perimeters, as measured by SC and K coefficients, resulted in values higher than 0.69 for SC and 0.68 for K, considering all case studies and the most accurate FARSITE simulations. In more detail, the best FARSITE simulations ranged from 0.69 to 0.86, in terms of SC, and from 0.68 to 0.82, in terms of K (Table 4). Concerning the simulation accuracy, FARSITE overestimations were expected and observed for all case studies (especially in YekeBermagh), since suppression activities were not considered in the simulations.

Overall, the simulations performed using the standard fuel models by Scott and Burgan (2005) provided better results than the Anderson fuel models (1982) in replicating the observed fire area, with the exception of the Malekroud case study

6217

(SC = 0.81; K = 0.78; Table 4). Among the fuel models, the best match between observed and modeled area burned was observed in tall grasslands (GR6; Scott and Burgan, 2005; Table 5), although also other fuel models (TU2, TU5 and TL9) provided very high accuracy, with SC $\geq$ 0.90 and K $\geq$ 0.82 (Table 5).

Simulation outputs for ROS, FLI and FML showed relatively moderate values for a number of fuel models. As expected, and according to the information provided by the Forest Brigades of the study areas, the highest spread rate and intensity values for the selected case studies were associated to grass and shrubs fuel models, which have high load and height. Specifically, the areas dominated by tall grass (GR6 and GR7) exhibited the highest rate of spread (ROS > 5 m min^{-1}; Table 5), with moderate intensity levels (FML < 2.5 m; Table 5): such fire behavior created strong difficulties for fire suppression mostly because of the high rate of spread, rather than the fire intensity. The limitations in effectively control fire spread rates were amplified in the areas where the terrain steepness was aligned with wind direction (e.g., Toshi wildfire, Fig. 8).

On the other hand, in timber litter and timber understory fuel models, the dead and live fuel moisture content is commonly higher than in open areas, the likelihood of fire ignition is much lower, and the spread rate and intensity do not present relevant complications for fire extinction if the fire spreads as surface fire, as observed in the case studies selected.

5 Conclusions

There are relevant effects of the fuel models characteristics on fine scale FARSITE outputs of fire spread and behavior. In the simulations performed for the fires events that affected northern Iranian forests, a wide variation of simulated fire perimeters, final size, rate of spread and intensity was observed. Overall, specific USDA standard fuel models were able to represent well the local vegetation conditions, which were mapped and defined combining field sampling activities and 1 : 25 000 land use maps. The best

6218

match between observed and simulated area burned was observed on grasslands fuel types.

Overall, fire modeling showed a high potential for estimating spatial variability in fire spread and behavior in the study areas. This work could represents a first step for the applications of fire spread modeling in Northern Iran for wildfire risk monitoring and management. Quantifying potential fire behavior, exposure and risk in Northern Iran, represents a challenging point for researchers, since the local fuels and fire data available for fire modeling are in the most of cases limited, and a huge work of field sampling and mapping is needed.

This work provides useful methodologies that can be replicated in the study areas to characterize fire likelihood and intensity and will increase local awareness of the risks posed by fire spreading in such forest ecosystems. Further efforts should be carried out to investigate crown fire behavior in the study areas, as well as to complete the field sampling in order to produce custom fuel models and photo-guides for northern Iran.

References

Adel, M. N., Pourbabaei, H., Omidi, A., and Pothier, D.: Long-term effect of fire on herbaceous species diversity in oriental beech (Fagus orientalis Lipsky) forests in Northern Iran, Forestry Studies in China, 14, 260–267, 2012.

Ager, A. A., Finney, M. A., Kerns, B. K., and Maffei, H.: Modeling wildfire risk to northern spotted owl (*Strix occidentalis caurina*) habitat in Central Oregon, USA, Forest Ecol. Manag., 246, 45–5, doi:10.1016/J.FORECO.2007.03.070, 2007.

Ager, A. A., Vaillant, N. M., and Finney, M. A.: A comparison of landscape fuel treatment strategies to mitigate wildland fire risk in the urban interface and preserve old forest structure, Forest Ecol. Manag., 259, 1556–1570, doi:10.1016/J.FORECO.2010.01.032, 2010.

Ager, A. A., Vaillant, N., and Finney, M. A.: Integrating Fire Behavior Models and Geospatial Analysis for Wildland Fire Risk Assessment and Fuel Management Planning, J. Combust., 2011, 19 pp., doi:10.1155/2011/572452, 2011.

Ager, A. A., Preisler, H., Arca, B., Spano, D., and Salis, M.: Wildfire risk estimation in the Mediterranean area, Environmetrics, 25, 384–396, doi:10.1002/env.2269, 2014a.

Ager, A., Buonopane, M., Reger, A., and Finney, M. A.: Wildfire exposure analysis on the national forests in the Pacific Northwest, USA, Risk Anal., 33, 1000–1020, 2014b.

Akhani, H.: Plant biodiversity of Golestan National Park, Iran, Stapfia, 53, 1–411, 1998.

Akhani, H. and Ziegler, H.: Photosynthetic pathways and habitats of grasses in Golestan National Park (NE Iran), with an emphasis on the C4-grass dominated rock communities, Phytocoenologia, 32, 455–501, 2002.

Akhani, H., Djamali, M., Ghorbanalizadeh, A., and Ramezani, E.: Plant biodiversity of Hyrcanian relict forests, N Iran: an overview of the flora, vegetation, palaeoecology and conservation, Pak. J. Bot., 42, 231–258, 2010.

Alexander, M. E. and Cruz, M. G.: Are the applications of wildland fire behaviour models getting ahead of their evaluation again?, Environ. Modell. Softw., 41, 65–71, 2013.

Anderson, H. E.: Aids to determining fuel models for estimating fire behaviour, General Technical Report INT-GTR-122, USDA Forest Service, Intermountain Forest and Range Experiment Station, United States Department of Agriculture, 1982.

Andrews, P. L., Heinsch, F. A., and Schelvan, L.: How to generate and interpret fire characteristics charts for surface and crown fire behavior, General Technical Report RMRS-GTR-253, USDA Forest Service, Rocky Mountain Research Station, Fort Collins, CO, 2011.

Arca, B., Duce, P., Laconi, M., Pellizzaro, G., Salis, M., and Spano, D.: Evaluation of FARSITE simulator in Mediterranean maquis, Int. J. Wildland Fire, 16, 563–572, 2007.

Arca, B., Bacciu, V., Pellizzaro, G., Salis, M., Ventura, A., Duce, P., Spano, D., and Brundu, G.: Fuel model mapping by IKONOS imagery to support spatially explicit fire simulators, in: 7th International Workshop on Advances in Remote Sensing and GIS Applications in Forest Fire Management towards an Operational Use of Remote Sensing in Forest Fire Management, Matera, Italy, 2–5 September, 4 pp., 2009.

Balbi, J. H., Morandini, F., Silvani, X., Filippi, J. B., and Rinieri, F. A.: Physical model for wildland fires, Combust. Flame, 156, 2217–2230, 2009.

Banj Shafiei, A., Akbarinia, M., Jalali, G., and Hosseini, M.: Forest fire effects in beech dominated mountain forest of Iran, Forest Ecol. Manag., 259, 2191–2196, 2010.

Bird, B. R., Bird, D. W., Codding, B. F., Parker, C. H., and Jones, J. H.: The "fire stick farming" hypothesis: Australian aboriginal foraging strategies, biodiversity, and anthropogenic fire mosaics, P. Natl. Acad. Sci. USA, 105, 14796–14801, 2008.

Boboulos, M., Purvis, M. R. I., and Penchev, S. I.: Fuel model development for the Greek East-Mediterranean forest litter layer, Fire Mater., 37, 597–611, doi:10.1002/fam.2159, 2013.

Bracmort, K.: Wildfire damages to homes and resources: understanding causes and reducing losses, Congressional Research Service (CRS), Washington, DC, 27 pp., 2012.

Byram, G. M.: Combustion of forest fuels, In: Forest Fire Control and Use, edited by: Davis, K. P., McGraw-Hill Book Company, New York, 61–89, 1956.

Cai, L., He, H. S., Wu, Z., Lewis, B. L., and Liang, Y.: Development of Standard Fuel Models in Boreal Forests of Northeast China through Calibration and Validation, PLoS ONE, 9, e94043, doi:10.1371/journal.pone.0094043, 2014.

Cardil, A., Molina, D. M., Ramirez, J., and Vega-García, C.: Trends in adverse weather patterns and large wildland fires in Aragón (NE Spain) from 1978 to 2010, Nat. Hazards Earth Syst. Sci., 13, 1393–1399, doi:10.5194/nhess-13-1393-2013, 2013.

Carvalho, J. P., Carola. M., and Tomé. J. A. B.: Forest fire modeling using rule-base fuzzy cognitive maps and voronoi based Cellular Automata, in: Annual Meeting of the North American Fuzzy Information Processing Society NAFIPS 2006, Montreal, QC, Canada, 3–6 June, 217–222, 2006.

Chuvieco, E., Yebra, M., Jurdao, S., Aguado, I., Salas, F. J., García, M., Nieto, H., De Santis, A., Cocero, D., Riaño, D., Martínez, S., Zapico, E., Recondo, C., Martínez-Vega, J., Martín, M. P., Riva, J., Pérez, F., and Rodríguez-Silva, F.: Field fuel moisture measurements on Spanish study sites, Department of Geography, University of Alcalá, Spain. Version 1, available at: http://www.geogra.uah.es/emilio/FMC_UAH.html, last access: September 2014, 2011.

Cochrane, M. A., Moran, C. J., Wimberly, M. C., Baer, A. D., Finney, M. A., Beckendorf, K. L., Eidenshink, J., and Zhu, Z.: Estimation of wildfire size and risk changes due to fuels treatments, Int. J. Wildland Fire, 21, 357–367, 2012.

Coleman, J. R. and Sullivan, A. L.: A real-time computer application for the prediction of fire spread across the Australian landscape, Simulation, 67, 230–240, 1996.

Congalton, R. G.: A review of assessing the accuracy of classifications of remotely sensed data, Remote Sens. Environ., 37, 35–46, doi:10.1016/0034-4257(91)90048-B, 1991.

Cruz, M. G. and Fernandes, P. M.: Development of fuel models for fire behavior prediction in maritime pine (*Pinus pinaster* Ait.) stands, Int. J. Wildland Fire, 17, 194–204, 2008.

Dimitrakopoulos, A. P.: Mediterranean fuel models and potential fire behavior in Greece, Int. J. Wildland Fire, 11, 127–130, 2002.

Djamali, M., de Beaulieu, J. L., Campagne, P., Andrieu-Ponel, V., Ponel, P., Leroy, S. A. G., and Akhani, H.: Modern pollen rain–vegetation relationships along a forest–steppe transect in the Golestan National Park, NE Iran, Rev. Palaeobot. Palyno., 153, 272–281, 2009.

Duguy, B., Alloza, J. A., Röder, A., Vallejo, R., Pastor, F.: Modeling the effects of landscape fuel treatments on fire growth and behaviour in a Mediterranean landscape (eastern Spain), Int. J. Wildland Fire, 16, 619–632, 2007.

FAO: Global Forest Resources Assessment, Progress Towards Sustainable Forest Management, Food and Agriculture Organization of the United Nations, Rome, 350 pp., 2005.

Fernandes, P., Luz, L., Loureiro, C., Ferreira-Godinho, P., and Botelho, H.: Fuel modelling and fire hazard assessment based on data from the Portuguese National Forest Inventory, Forest Ecol. Manag., 234, S229, doi:10.1016/j.foreco.2006.08.256, 2006.

Fernandes, P. M.: Examining fuel treatment longevity through experimental and simulated surface fire behaviour: a maritime pine case study, Can. J. Forest Res., 39, 2529–2535, 2009.

Filippi, J.-B., Mallet, V., and Nader, B.: Evaluation of forest fire models on a large observation database, Nat. Hazards Earth Syst. Sci. Discuss., 2, 3219–3249, doi:10.5194/nhessd-2-3219-2014, 2014.

Finney, M. A.: FARSITE: fire area simulator – model development and evaluation, Res. Pap. RMRS-RP-4, US Department of Agriculture, Forest Service, Rocky Mountain Research Station, Ogden, UT, 1998.

Finney, M. A.: Design of regular landscape fuel treatment patterns for modifying fire growth and behavior, Forest Sci., 47, 219–228, 2001.

Finney, M. A.: Calculation of fire spread rates across random landscapes, Int. J. Wildland Fire, 12, 167–174, 2003.

Finney, M. A. and Ryan, K. C.: Use of the FARSITE fire growth model for fire prediction in the US national parks, in: International Emergency Management and Engineering Conference, Nice,

France, 9–12 May 1995, edited by: Sullivan, J. D., Wybo, J. L., and Buisson, L., TIEMES, Dallas, TX, 183–189, 1995.

Finney, M. A., Seli, R. C., McHugh, C. W., Ager, A. A., Bahro, B., and Agee, J. K.: Simulation of long-term landscape-level fuel treatment effects on large wildfires, in: Fuels Management – How to Measure Success: Conference Proceedings, Portland, OR, 28–30 March, edited by: Andrews, P. L., and Butler, B. W., USDA Forest Service, Rocky Mountain Research Station Proceedings RMRS-P-41, 125–148, 2006.

Finney, M. A., Grenfell, I. C., McHugh, C. W., Seli, R. C., Trethewey, D., Stratton, R. D., and Brittain, S.: A method for ensemble wildland fire simulation, Environ. Model. Assess., 16, 153–167, 2011.

Forthofer, J. and Butlerm, B.: Differences in simulated fire spread over Askervein Hill using two advanced wind models and a traditional uniform wind field, USDA Forest Service Proceedings RMRS-P-46, U.S. Department of Agriculture, Forest Service, Rocky Mountain Research Station, 2007.

Glasa, J. and Halada, L.: A note on mathematical modelling of elliptical fire propagation, Comput. Inform., 30, 1303–1319, 2011.

Gu, F., Hu, X., and Ntaimo, L.: Towards validation of DEVS-FIRE wildfire simulation model, in: Proceedings of the 2008 Spring Simulation Multiconference, Ottawa, Canada, 355–361, 2008.

Hardison, T.: Application of Remote Sensing and GIS to modelling fire for vegetative restoration in Northern Arizona, MSc Thesis (Biology), University of NorthTexas, USA, 57 pp., 2003.

Keeley, J. E. and Fotheringham, C. J.: The historical role of fire in California shrublands, Conserv. Biol., 15, 1536–1548, 2001.

LaCroix, J. J., Ryu, S. R., Zheng, D., and Chen, J.: Simulating fire spread with landscape management scenarios, For. Sci., 52, 522–529, 2006.

Lee, H., Limb, S., and Paikc, H.: An assessment of fire-damaged forest using spatial analysis techniques, J. Spat. Sci., 55, 289–301, 2010.

Leestmans, R.: Le refuge caspien et son importance en biogéographie, Linneana Belgica, 10, 97–102, 2005 (in French).

Legendre, P. and Legendre, L.: Numerical Ecology, 2nd Edn., Elsevier, Amsterdam, 1998.

Leroy, A. G. S. and Arpe, K.: Glacial refugia for summer-green trees in Europe and south-west Asia as proposed by ECHAM3 time-slice atmospheric model simulations, J. Biogeogr., 34, 2115–2128, 2007.

6223

Mallinis, G., Mitsopoulos, I. D., Dimitrakopoulos, A. P., Gitas, I. Z., and Karteris, M.: Local-scale fuel-type mapping and fire behaviorprediction by employing high-resolutionsatellite imagery, IEEE J. Sel. Top. Appl., 1, 230–239, 2008.

Marshall, P. L., Davis, G., and LeMay, V. M.: Using line intersect sampling for coarse woody debris, tecnical report TR-003, Research Section, Vancouver Forest Region, British Columbia Ministry of Forests, Canada, 37 pp., 2000.

Marshall, P. L., Davis, G., and Taylor, S.: Using line intersect sampling for coarse woody debris: practitioner's questions addressed, Note EN-012, Vancouver Forest Region Extension, Ministry of Forests, Canada, pp. 10, 2003.

Martinez, J., Vega-Garcia, C., and Chuvieco, E.: Human-caused wildfire risk rating for prevention planning in Spain, J. Environ. Manage., 90, 1241–1252, 2009.

Marvi Mohadjer, M.: Silviculture, University of Tehran Press, Tehran, Iran, 387 pp., 2005 (in Persian).

Mendes-Lopes, J. and Aguas, C.: SPREAD – Un programa de Automatos Celulares para Propagaçao de Fogos Florestais, Silva Lusitana, 8, 3–47, 2000.

Mirdeylami, T., Shataee, S., and Kavousi, M. R.: Forest fire risk zone mapping in the Golestan national park using weighted linear combination (WLC) method, Iranian Journal of Forest, 5, 377–390, 2014 (in Persian).

Molina, D. M. and Castellnou, M.: Wildland fuel management in Catalonia (NE Spain), in: Actes de la 1ère Conférence Internationale sur les Stratégies de Prévention des Incendies dans les Forêts d'Europe du Sud, 31 January–2 February 2002, Bordeaux, France, Préventique, Bordeaux, 95–102, 2002.

Opperman, T., Gould, J., Finney, M., and Tymstra, C.: Applying fire spread simulators in New Zealand and Australia: results from an international seminar, in: Fuels Management-How to Measure Success: Conference Proceedings. 28-30 March 2006; Portland, OR. Proceedings RMRS-P-41, edited by: Andrews, P. L. and Butler, B. W., U.S. Department of Agriculture, Forest Service, Rocky Mountain Research Station, Fort Collins, CO, 201–212, 2006.

Pausas, J. G., Llovet, J., Rodrigo, A., and Vallejo, R.: Are wildfires a disaster in the Mediterranean basin? – A review, Int. J. Wildland Fire, 17, 713–723, 2008.

Pettinari, M. L., Ottmar, R. D., Prichard, S. J., Andreu, A. G., and Chuvieco, E.: Development and mapping of fuel characteristics and associated fire potentials for South America, Int. J. Wildland Fire, 23, 643–654, 2013.

6224

Pierce, D., McDaniel, S., Wasser, M., Ainsworth, A., Litton, C. M., Giardina, C. P., and Cordell, S.: Using a prescribed fire to test customand standard fuel models for fire behavior prediction in a non-native, grass-invaded tropical dry shrubland, Appl. Veg. Sci., 17, 700–710, doi:10.1111/avsc.12111, 2014.

5 Prometheus Project Steering Committee: Development and Application of a Wildland Fire Growth Model. Proposal to Foothills Model Forest, Canadian Forest Service, 28 pp., 1999.

Randall, D. A., Wood, R. A., Bony, S., Colman, R., Fichefet, T., Fyfe, J., Kattsov, V., Pitman, A., Shukla, J., Srinivasan, J., Stouffer, R. J, Sumi, A., and Taylor, K. E.: Climate models and their evaluation, in: Climate Change 2007: The Physical Science Basis. Contribution of

10 Working Group I to the Fourth Assessment Report of the Intergovernmental Panel on Climate Change, edited by: Solomon, S., Qin, D., Manning, M., Chen, Z., Marquis, M., Averyt, K. B., Tignor, M., and Miller, H. L., Cambridge University Press, Cambridge, UK, 589–662, 2007.

Rodríguez y Silva, F. and Molina-Martínez, J. R.: Modelling Mediterranean forest fuels by integrating field data and mapping tools, Eur. J. For. Res., 131, 571–582,

15 doi:10.1007/s10342-011-0532-2, 2011.

Romero-Calcerrada, R., Novillo, C., Millington, J. D. A., and Gomez-Jimenez, I.: GIS analysis of spatial patterns of human-caused wildfire ignition risk in the SW of Madrid (Central Spain), Landscape Ecol., 23, 341–354, 2008.

Rothermel, R. C.: A Mathematical Model for Predicting Fire Spread in Wildland Fuels, USDA

20 Forest Service Research Paper, INT-115, Intermountain Forest and Range Experiment Station, Ogden, UT, 1972.

Rothermel, R. C.: How to Predict the Spread and Intensity of Forest and Range Fires, National Wildlife Coordinating Group, Boise, ID, 1983.

Ryu, S. R., Chen, J., Zheng, D., and LaCroix, J. J.: Relating surface fire spread to landscape

25 structure: an application of FARSITE in a managed forest landscape, Landscape Urban Plan., 83, 275–283, 2007.

Sağlam, B., Bilgili, E., Küçük, O., and Durmaz, B. D.: Fire behavior in Mediterranean shrub species (Maquis), Afr. J. Biotechnol., 7, 4122–4129, 2008.

Salis, M.: Fire Behavior Simulation in Mediterranean Maquis Using FARSITE (Fire Area

30 Simulator), Ph.D. Thesis, Università degli Studi di Sassari, Dipartimento di Economia e Sistemi Arborei, Sassari, Italy, 130 pp., 2008.

Salis, M., Arca, B., Bacciu, V., Spano, D., Duce, P., Santoni, P., Ager, A., and Finney, M.: Application of wildfire spread and behavior models to assess fire probability and severity

in the Mediterranean region, EGU General Assembly, Vienna, Austria, 2–7 May 2010, Geophysical Research Abstracts, 12, EGU2010-12991, 2010.

Salis, M., Ager, A. A., Arca, B., Finney, M. A., Bacciu, V., Duce, P., and Spano, D.: Assessing exposure of human and ecological values to wildfire in Sardinia, Italy, Int. J. Wildland Fire,

5 22, 549–565, 2013.

Salis, M., Ager, A. A., Arca, B., Finney, M. A., Alcasena, F., Bacciu, V., Duce, P., Lozano, O. M., and Spano, D.: Analyzing wildfire exposure on Sardinia, Italy, EGU General Assembly, Vienna, Austria, 27April–2 May 2014, Geophysical Research Abstracts, 16, EGU2014-11596, 2014a.

10 Salis, M., Ager, A. A., Finney, M. A., Arca, B., and Spano, D.: Analyzing spatiotemporal changes in wildfire regime and exposure across a Mediterranean fire-prone area, Nat. Hazards, 71, 1389–1418, 2014b.

Santoni, P. A. and Balbi, J. H.: Modelling of two dimensional flame spread across a sloping fuel bed, Fire Safety J., 31, 201–225, 1998.

15 Santoni, P. A., Filippi, J. B., Balbi, J. H., and Bosseur, F.: Wildland fire behaviour case studies and fuel models for landscape-scale fire modeling, J. Combust., 2011, 613424, doi:10.1155/2011/613424, 2011.

Sarkargar Ardakani, A.: Analysis of radiometric-spatial characteristics of fire and its Application in identification and separation by remote sensing data, Ph.D. thesis, Faculty of Engineering,

20 Khaje-Nasir-Toosi University, Tehran, Iran, 290 pp., 2007 (in Persian).

Schmidt, D. A., Taylor, A. H., and Skinner, C. N.: The influence of fuels treatment and landscape arrangement on simulated fire behavior, Southern Cascade range, California, Forest Ecol. Manag., 255, 3170–3184, 2008.

Scott, J. H. and Burgan, R.: Standard Fire Behavior Fuel Models: a Comprehensive Set for Use

25 with Rothermel's Surface Fire Spread Model, RMRS-GTR-153, USDA Forest Service, Rocky Mountain Research Station, Fort Collins, CO, 2005.

Sharples, J. J., McRae, R. H. D., and Wilkes, S. R.: Wind–terrain effects on the propagation of wildfires in rugged terrain: fire channelling, Int. J. Wildland Fire, 21, 282–296, 2012.

Siadati, S., Moradi, H., Attari, F., Etemad, V., Hamzeh'ee, B., and Naqinezhad, A.: Botanical

30 diversity of Hyrcanian forests; a case study of a transect in theKheyrud protected lowland mountain forests in Northern Iran, Phytotaxa, 7, 1–18, 2010.

Stephens, S. L.: Evaluation of the effects of silvicultural fuels treatments on potential fire behaviour in Sierra Nevada mixed-conifer stands, Forest Ecol. Manag., 105, 21–35, doi:10.1016/S0378-1127(97)00293-4, 1998.

5 Stratton, R. D.: Assessing the effectiveness of landscape fuel treatments on fire growth and behavior, J. Forest., 102, 32–40, 2004.

Stratton, R. D.: Guidance on Spatial Wildland Fire Analysis: Models, Tools, and Techniques, Gen. Tech. Rep. RMRS-GTR-183, US Department of Agriculture, Forest Service, Rocky Mountain Research Station, Fort Collins, CO, 15 pp., 2006.

Syphard, A. D., Radeloff, V. C., Keeley, J. E., Hawbaker, T. J., Clayton, M. K., Stewart, S. I., and

10 Hammerm, R. B.: Human influence on California fire regimes, Ecol. Appl., 17, 1388–1402, 2007.

Sullivan, A.: Wildland surface fire spread modelling, 1990–2007. 2: Empirical and quasiempirical models, Int. J. Wildland Fire, 18, 369–386, 2009.

Taylor, S. W., Woolford, D. G., Dean, C. B., and Martell, D. L.: Wildfire prediction to inform

15 firemanagement: statistical science shallenges, Stat Sci., 28, 586–615, 2013.

Viegas, D. X., Ribeiro, P. R., and Maricato, L.: An empirical model for the spread of a fireline inclined in relation to the slope gradient or to wind direction, in: Proceeding of the Third International Conference on Forest Fire Research, vol. 2718, edited by: Viegas, D. X., University of Coimbra, Coimbra, Portugal, 325–342, 1998.

20 Zarekar, A., Kazemi Zamani, B., Ghorbani, S., Ashegh Moalla, M., and Jafari, H.: Mapping spatial distribution of forest fire using MCDM and GIS, case study: three forest zones in Guilan province, Iranian Journal of Forest and Poplar Research, 21, 218–230, 2013 (in Persian).

6227

Table 1. Case study sites description.

Site	Siahkal		GNP	
Wildfire	Toshi	Malekroud	YekeBermagh	Gharangi
Latitude	37°11′	37°03′	37°22′	37°21′
Longitude	49°88′	49°84′	56°03′	56°02′
Elevation (m)	210	120	2080	1370
Main fuel types affected by the fire	grasslands, grass-shrublands and timber understory	timber litter	Grasslands and grass-shrublands	timber understory and timber litter
Dominant plant species	*Carpinus betulus* L., *Quercus castaneifolia* C.A. Mey., *Alnus subcordata* C.A. Mey., *Parrotia persica* C.A. Mey., *Acer insigne var. velutinum* Boiss., *Asperula odorata* L., *Euphorbia helioscopia* L., *Ilex aquifolium* L.	*Acer insigne var. velutinum* Boiss., *Quercus castaneifolia* C.A. Mey., *Fagus orientalis* C.A. Mey., *Populus caspica* C.A. Mey., *Tilia begonifolia* Stev., *Pyrus commonis* L., *Buxus hyrcanus* Pojark., *Mespilus germanica* L., *Smilax excelsa* L., *Hypricum androsenum* L.	*Festuca drymeia* Mert. & Koch., *Artemisia sieberi* Besser., *Astragalus jolderensis* B. Fedtsch., *Poa bulbosa* L., *Thymus kotschyanus* Boiss. & Hohen., *Stipa holosericea* Trin., *Juniperus excelsa* M. Bieb., *Juniperus communis* L.	*Quercus castaneifolia* C.A. Mey., *Carpinus betulus* L., *Carpinus orientalis* Mill., *Acer cappadocicum* Gled., *Mespilus germanica* L., *Euphorbia amygdaloides* L., *Viola alba* Besser., *Primula heterochroma* Stapf., *Galium odoratum* (L.) Scop.
Fire ignition (date and hour)	14 Aug 2010 (16:00)	17 Dec 2010 (17:00)	15 Jul 2011 (11:00)	28 Mar 2011 (14:00)
Fire extinguishment (date and hour)	15 Aug 2010 (17:00)	18 Dec 2010 (08:00)	15 Jul 2011 (21:00)	28 Mar 2011 (21:00)
Burned area (ha)	34	24	60	10

6228

Table 2. Overview of the weather conditions observed during the wildfire days in the closest weather stations.

Site Wildfires	Siahkal[a]		GNP[b]	
	Toshi	Malekroud	YekeBermagh	Gharangi
Maximum Temperature (°C)	35	25	31	17
Minimum Temperature (°C)	20	7	14	5
Precipitation (mm)	0	0	0	0
Maximum Wind Speed (km h^{-1})	28.8	32.4	25.2	18.0
Average Wind Speed (km h^{-1})	21.6	23.4	21.6	14.4
Average Wind Direction	NE	S	SW	SE
Average Air Relative Humidity (%)	50	58	21	49

[a] Lahijan Station (−2 m) (lat. 37°11′, long. 50°00′), located 15 km away from the northeast of Siahkal forest area.
[b] Dasht-Golestan climatology station (1000 m a.s.l.) (lat. 37°17′, long. 56°01′) and Robate-GharehBil automatic weather station (1282 m a.s.l.) (lat. 37°21′, long. 56°19′), located 7 and 20 km away from the south and east boundaries of GNP, respectively.

Table 3. Fuel types and respective fuel models and fuel moisture parameters used in FARSITE simulations.

Wildfire	Vegetation Type	Fuel Models by Scott and Burgan (2005)	Fuel Models by Anderson (1982)	FMC (%)				
				Dead Fuel (%)			Live Fuel (%)	
				1 h	10 h	100 h	LH	LW
Toshi	Grassland	GR5, GR6	FM3	11	12	14	0	0
	Grass–Shrubland	GS3	FM5, FM6	11	12	14	0	70
	Natural Mixed Forest	TU2, TU3	FM9, FM10	11	12	14	0	100
Malekroud	Mixed and Pure Plantation	TL2, TL6, TL8, TL9	FM9, FM10	14	15	17	50	100
YekeBermagh	Grassland	GR1, GR2, GR4, GR7	FM1, FM2	5	6	8	0	0
	Grass–Shrubland	GS1, GS2	FM5, FM6	5	6	8	0	60
	Shrubland	SH1, SH2	FM5, FM6	5	6	8	0	70
Gharangi	Natural Mixed Forest	TU1, TU5	FM8, FM10	13	14	16	75	100
	Natural Pure Forest	TL2, TL6, TL9	FM9, FM10	13	14	16	75	100

Table 4. Statistical evaluation of FARSITE performance for different combinations of standard fuel models. The values of the best FARSITE simulations are in bold. The Sorensen's coefficient (SC) and the Cohen's kappa coefficient (K), derived from the error matrix; were used for such purpose. (a) burned area agreement; (b) FARSITE overestimation; (c) FARSITE underestimation.

Site	Simulation Number	Fuel Model code	SC	K	a (ha)	b (ha)	c (ha)
Toshi	**I**	**(GR6, GS3, TU2, TU3)**	**0.86**	**0.82**	**30.06**	**5.51**	**4.12**
	II	(FM3, GS3, TU2, TU3)	0.81	0.78	17.08	4.53	3.14
	III	(GR6, FM5, TU2, TU3)	0.77	0.74	11.06	3.97	2.44
	IV	(GR6, GS3, FM10, TU3)	0.78	0.75	9.49	1.39	3.73
	V	(GR6, GS3, TU2, FM10)	0.81	0.79	10.88	2.61	2.34
	VI	(FM3, FM6, FM10, FM10)	0.70	0.67	8.40	0.39	6.82
	VII	(GR6, GS3, FM9, TU3)	0.48	0.45	4.80	0.05	10.42
Malekroud	I	(TL6, TL9)	0.76	0.73	17.18	4.13	6.87
	II	**(FM9, TL9)**	**0.81**	**0.78**	**20.57**	**5.51**	**3.48**
	III	(TL6, FM9)	0.75	0.73	16.95	4.01	7.10
	IV	(TL6, FM10)	0.73	0.71	15.84	3.48	8.21
	V	(FM9, FM9)	0.78	0.75	19.45	5.60	4.80
YekeBermagh	I	(GR7, GS1, GS2)	0.24	0.20	58.06	358.90	0.00
	II	(GR4, GS1, GS2)	0.26	0.22	58.06	326.48	0.00
	III	(FM1, GS1, GS2)	0.41	0.38	58.06	165.91	0.00
	IV	(FM2, GS1, GS2)	0.65	0.63	51.43	45.86	8.63
	V	**(GR4, SH1, SH2)**	**0.69**	**0.68**	**46.84**	**30.75**	**11.22**
	VI	(FM2, SH1, SH2)	0.13	0.12	4.26	3.27	53.80
	VII	(FM2, FM5, FM6)	0.67	0.66	50.14	41.67	7.92
	VIII	(GR4, FM5, FM6)	0.27	0.23	58.06	308.65	0.00
Gharangi	**I**	**(TU1, TU5, TL6, TL9)**	**0.76**	**0.75**	**7.48**	**2.23**	**2.56**
	II	(FM8, TU5, TL6, TL9)	0.67	0.65	7.50	4.81	2.54
	III	(FM10, TU5, TL6, TL9)	0.57	0.56	8.44	11.30	1.60
	IV	(TU1, FM10, TL6, TL9)	0.71	0.69	7.03	1.53	4.01
	V	(TU1, TU5, FM9, TL9)	0.71	0.68	7.31	2.24	3.73
	VI	(TU1, TU5, TL6, FM10)	0.70	0.69	6.63	2.19	3.41
	VII	(FM8, FM10, FM9, FM10)	0.70	0.69	6.79	2.54	3.25

Table 5. Statistical evaluation of the best FARSITE simulations (I for Toshi, II for Malekroud, V for YekeBermagh and I for Gharangi; Table 5) for each case study. Mean values (±SE) of the simulated ROS, FLI and FML are also reported. (SC = Sorensen's coefficient value; K = Cohen's kappa coefficient value; a = burned area agreement; b = FARSITE overestimation; c = FARSITE underestimation; ROS = rate of spread; FLI = fire line intensity; FML = flame length).

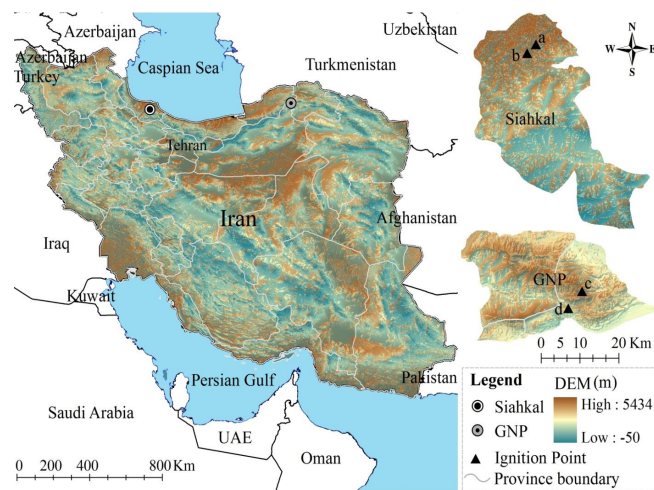| Site	Fuel Model	SC	K	a (ha)	b (ha)	c (ha)	Wildfire Area (ha)	Simulated Area (ha)	ROS (m min^{-1})	FLI (kW m^{-1})	FML (m)
Toshi	106 GR6	0.92	0.87	12.87	2.11	0.27	13.14	15.25	3.94 ± 2.49	655.62 ± 418.38	1.44 ± 0.46
	123 GS3	0.87	0.85	3.98	0.43	0.70	4.68	5.11	1.20 ± 0.38	169.26 ± 63.80	0.80 ± 0.16
	162 TU2	0.90	0.82	6.28	0.07	1.35	7.63	7.70	0.58 ± 0.31	46.44 ± 41.72	0.42 ± 0.14
	163 TU3	0.75	0.73	6.93	2.90	1.80	8.73	11.63	1.61 ± 1.55	239.38 ± 261.60	0.88 ± 0.42
	Total	0.86	0.82	30.06	5.51	4.12	34.18	39.69	2.27 ± 2.23	357.65 ± 383.74	1.01 ± 0.53
Malekroud	FM9	0.85	0.82	16.12	3.19	2.80	18.92	22.11	1.76 ± 0.78	126.35 ± 56.01	0.69 ± 0.14
	189 TL9	0.77	0.74	4.45	2.32	0.68	5.13	7.45	1.62 ± 0.75	262.96 ± 155.09	0.95 ± 0.30
	Total	0.81	0.78	20.57	5.51	3.48	24.05	29.56	1.72 ± 0.78	160.63 ± 108.19	0.76 ± 0.23
YekeBermagh	104 GR4	0.82	0.81	42.05	19.93	5.82	47.87	61.98	2.60 ± 1.28	341.26 ± 255.52	1.01 ± 0.39
	141 SH1	0.75	0.72	3.29	5.39	2.52	5.81	8.68	2.83 ± 1.09	266.89 ± 113.11	0.95 ± 0.19
	142 SH2	0.50	0.50	1.50	5.43	2.88	4.38	6.93	1.49 ± 1.63	248.52 ± 234.96	0.58 ± 0.56
	Total	0.69	0.68	46.84	30.75	11.22	58.06	77.59	2.61 ± 1.36	277.86 ± 416.89	0.97 ± 0.70
Gharangi	161 TU1	0.47	0.45	0.90	0.82	2.18	3.08	3.90	0.32 ± 0.29	85.55 ± 118.41	0.45 ± 0.36
	165 TU5	0.90	0.85	3.52	0.52	0.30	3.82	4.34	0.67 ± 0.24	205.75 ± 115.23	0.86 ± 0.22
	186 TL6	0.77	0.77	0.95	0.49	0.08	1.03	1.52	0.23 ± 0.04	23.99 ± 24.38	0.32 ± 0.09
	189 TL9	0.91	0.91	2.11	0.40	0	2.11	2.51	0.63 ± 0.19	149.43 ± 83.11	0.74 ± 0.20
	Total	0.76	0.75	7.48	2.23	2.56	10.04	12.27	0.53 ± 0.28	184.43 ± 147.94	0.76 ± 0.37

Figure 1. Location of the sites where the four fire events occurred, in northern Iran: (a) Toshi and (b) Malekroud, in Siahkal forest area; (c) YekeBermagh and (d) Gharangi, in Golestan National Park (GNP).
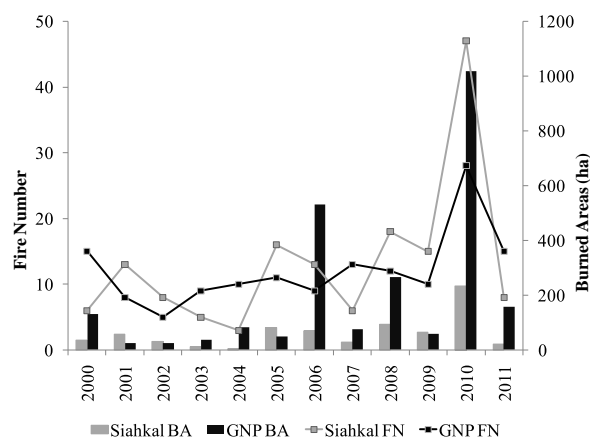
Figure 2. Fire number (FN) and burned area (BA) in Siahkal forest area and GNP (2000–2011; data from Department of Forestry, Natural Resources Office, Guilan, and Department of Environment, Golestan, Iran, personal communication, 2011, 2012).

Figure 3. Monthly fire number (FN) and burned area (BA) in Siahkal forest area and GNP (2000–2011; data from Department of Forestry, Natural Resources Office, Guilan, and Department of Environment, Golestan, Iran, personal communication, 2011, 2012).

6235

Figure 4. Historical relationship between fire size categories and percentage of fire number (FN) and burned area (BA) in Siahkal forest area and GNP (2000–2011; data from Department of Forestry, Natural Resources Office, Guilan, and Department of Environment, Golestan, Iran, personal communication, 2011, 2012).
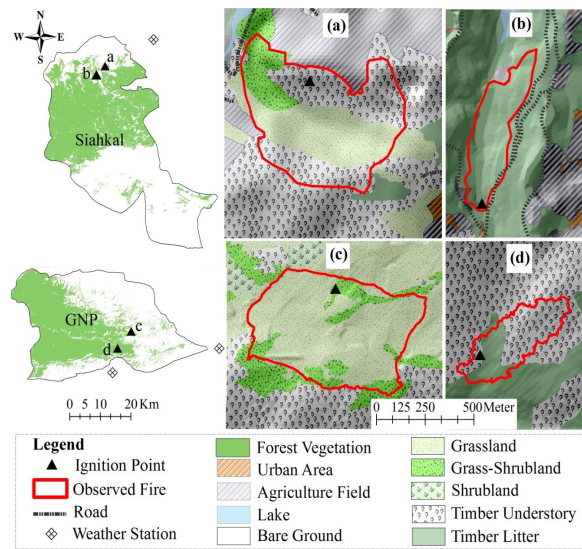
Figure 5. Vegetation maps of the sites where the selected fire events occurred: **(a)** Toshi and **(b)** Malekroud in Siahkal forest area; **(c)** YekeBermagh and **(d)** Gharangi in GNP. The nearest weather stations to the fire events are presented in the map.
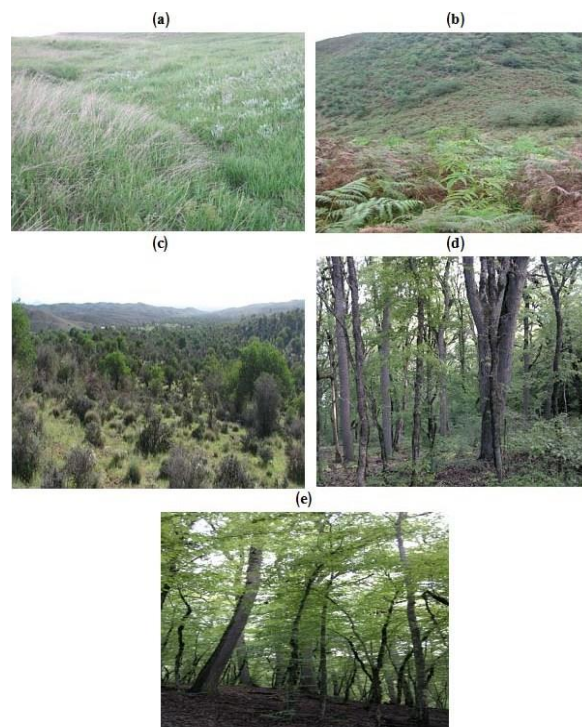
6237

Figure 6. Photo guide of the main fuel types of the study areas: **(a)** grassland fuel types, **(b)** grass-shrublands fuel types, **(c)** shrubby fuel types, **(d)** natural mixed timber understory fuel types, **(e)** broadleaf timber litter fuel types.
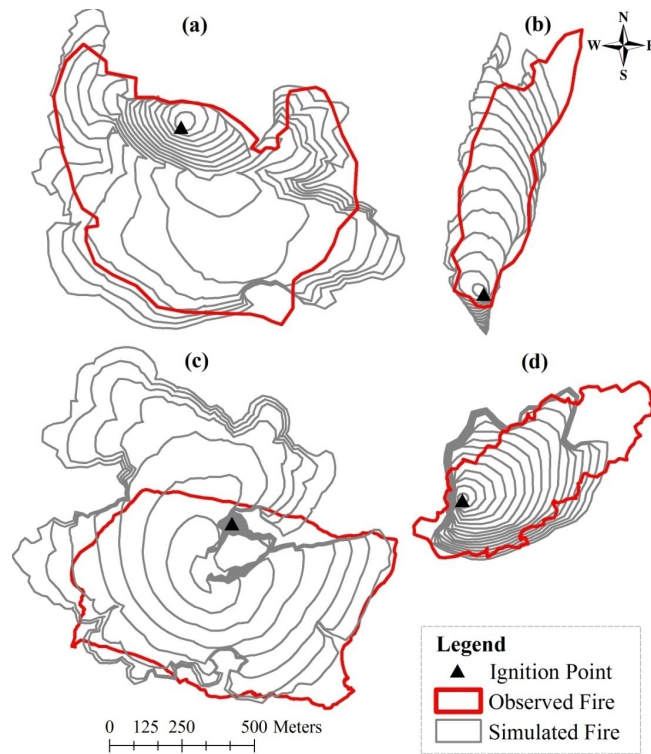
6238

Figure 7. Fire spread perimeters (30 min interval) simulated by FARSITE (gray) vs. actual fire perimeters (red): **(a)** Toshi, **(b)** Malekroud, **(c)** YekeBermagh, **(d)** Gharangi.
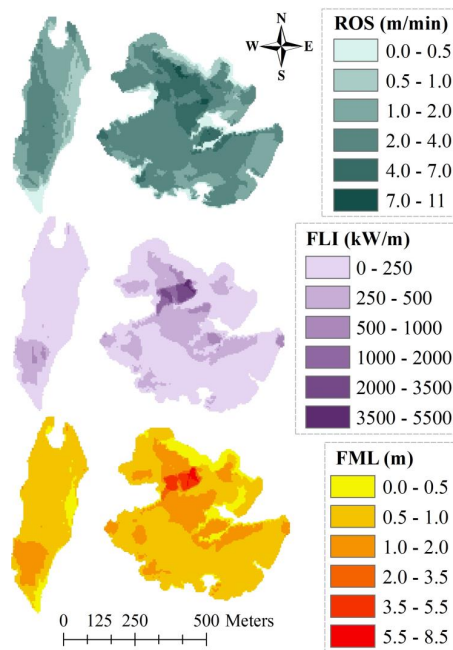
Figure 8. Simulated outputs of rate of spread (ROS), fireline intensity (FLI) and flame length (FML) for the case studies of Malekroud (left) and YekeBermagh (right).